ISSN 1063-780X, Plasma Physics Reports, 2025, Vol. 51, No. 8, pp. 897–905. © The Author(s), 2025. This article is an open access publication.

INTERACTION OF WAVES WITH PLASMA

Determination of Conditions for Efficient Excitation of Fast Magnetosonic Waves in Plasma of the L-2M Stellarator in Ohmic Heating Regime

A. I. Meshcheryakov[a,*], I. A. Grishina[a], M. E. Popov[a,c], K. O. Nedbailov[d], V. A. Shapkin[a], A. A. Letunov[a], V. P. Logvinenko[a,b], V. D. Stepakhin[a], D. G. Vasilkov[a], N. G. Gusein-zade[a], A. M. Davydov[a], V. A. Ivanov[a,c], M. A. Tereshchenko[a], and N. K. Kharchev[a]

[a] *Prokhorov General Physics Institute, Russian Academy of Sciences, Moscow, 119991 Russia*

[b] *RUDN University, Moscow, 117198 Russia*

[c] *National Research Nuclear University "MEPhI," Moscow, 115409 Russia*

[d] *National Research Centre "Kurchatov Institute," Moscow, 123098 Russia*

**e-mail: meshch@fpl.gpi.ru*

Received July 16, 2025; revised August 18, 2025; accepted August 20, 2025

Abstract—The system of magnetic probes and data acquisition system have been developed and created at the L-2M stellarator for measuring phase velocities of fast magnetosomic (FMS) waves. Using this system of magnetic probes, toroidal and azimuthal wave numbers of FMS waves excited in the L-2M stellarator plasma were determined in the ohmic heating regime at 1-kW-power of radiation introduced into the plasma, plasma densities in the range of $(0.5–2.0) \times 10^{19}$ m^{-3} and magnetic fields in the range of 1–1.4 T. The conditions for the density and magnetic field strength under which FMS wave can propagate in one of the toroidal directions in the L-2M stellarator plasma were determined in the ohmic heating regime.

Key words: ion cyclotron heating, fast magnetosonic waves, magnetic probes, L-2M stellarator, simulations of propagation of fast magnetosonic waves, ohmic heating regime

DOI: 10.1134/S1063780X25603219

1. INTRODUCTION

Implementation of controlled fusion reaction in plasma is one of the possible ways for providing modern civilization with new energy resources, as well as producing neutrons for industrial and medical needs. At present, tokamak seems to be the most likely type of facilities with magnetic plasma confinement, on the basis of which the first industrial fusion reactor will be created. When developing such a reactor, one of the main problems is maintaining the stationary plasma current. In tokamaks, the plasma current is created inductively, and, therefore, it cannot be maintained stationary for unrestrictedly long time. In future fusion reactors, the stationary current is planned to be maintained by non-inductive methods, including current drive.

Currently, active search for the most efficient methods for current drive is underway at operating toroidal facilities. The current drive efficiency is determined by the following expression

$$\eta_{CD} = Rn_e I_{CD}/P_{abs}, \quad (1)$$

where R is the major radius of facility in meters, n_e is the average plasma density in units of 10^{19} m^{-3}, I_{CD} is the driven current in Amperes, and P_{abs} is the absorbed RF power in Watts [1].

Lower Hybrid Current Drive (LHCD) by waves in the frequency range of 1–10 GHz is the most successful method among the radio-frequency methods for current drive. Within the framework of this method, slow waves are excited in plasma using grill launchers, which propagate towards the center of the plasma column, where they are absorbed by electrons in the lower hybrid resonance region. For waves in this frequency range, there is an opacity region at the edge of the plasma column. The wave can overcome this opacity zone only if the magnetic field of the facility will be increased.

The highest LHCD efficiency (3.5×10^{19} m^{-2} A/W) was reached at the JT-60U tokamak [2] at the magnetic field of 5 T. The highest for toroidal magnetic traps driven current of 3.6 MA was also obtained at this facility. These values are record-breaking for experiments on current drive using all known methods. Successful experiments on LHCD were also performed at

the ALCATOR-C tokamak at the magnetic field of 8 T, in which the current drive efficiency was 2.5×10^{19} m^{-2} A/W [3]. The LHCD method is quite efficient, but has fundamental limitations on plasma density associated with the existence of opacity region for slow waves at the plasma edge. For each specific facility, this limit is determined by the magnitude of the toroidal magnetic field.

Another method for current drive in plasma, which is currently being investigated at toroidal facilities, is the electron cyclotron current drive (ECCD) by waves in the range of electron cyclotron frequencies (20–200 GHz). Such experiments were conducted at the T-10 and DIII-D tokamaks. Since waves excited in plasma are absorbed in accordance with the cyclotron mechanism, the wave energy increases the transverse (relative to the direction of the magnetic field) velocity of electrons. Therefore, the ECCD efficiency along the magnetic field direction is lower, as compared to that of the LHCD method. For example, in experiments at the T-10 tokamak [4], the ECCD efficiency, calculated using formula (1), was 0.075×10^{19} m^{-2} A/W at the electron temperature of 4 keV. In similar experiments at the DIII-D tokamak [5], the ECCD efficiency was 0.19×10^{19} m^{-2} A/W at the higher electron temperature of ~7 keV.

Research on current drive by waves in the ion cyclotron frequency range is also being conducted at tokamaks. Experiments on current drive by fast magnetosonic (FMS) waves with frequencies in the range of 60–83 MHz had been conducted at the DIII-D tokamak [6]. In this experiment, by changing phase relations between three radiating antennas, excitation and propagation of FMS waves along the direction of plasma current or in the opposite direction was demonstrated. The FMS waves were absorbed by electrons due to the Landau damping mechanism. In this experiment, the current drive efficiency was 0.54×10^{19} m^{-2} A/W. The efficiency of this method turns out to be low because the absorption of FMS waves due to the Landau damping mechanism is rather weak in plasmas of currently operating toroidal facilities. Due to the small sizes of facilities and insufficiently high electron temperatures, the number of electrons with velocities comparable with the wave phase velocity is small.

There is one more method for current drive using FMS waves, which consists in converting FMS waves into slow waves with their subsequent absorption by electrons due to the Landau damping mechanism. The efficiency of this method should be higher than that of the method based on direct absorption of FMS waves, since thermal electrons will participate in this process, but not electrons from the "tail" of the electron energy distribution. Experiments on current drive using this method were performed at the TFTR tokamak [7]. Conversion of FMS waves into the Bernstein mode was carried out in deuterium plasma with ^{3}He and ^{4}He minorities at the frequency of 43 MHz. In the experiment, up to 80% of the heating power introduced into the plasma was absorbed by the electron component. Simulations using the FELICE code showed that high fraction of introduced power (up to 80–90%) is absorbed by electrons near the mode conversion surface. At the L-2M stellarator, it is also planned to conduct experiments on mode conversion current drive using FMS waves, and they will be conducted in deuterium plasma with hydrogen minority.

Currently, current drive scenarios using the conversion of FMS waves into slow waves are actively simulated worldwide (for example, for the EAST tokamak [8, 9]). This method for current drive is called MCCD (Mode-Conversion Current Drive). In [9], for the EAST facility, the RF power absorbed by electrons during the conversion of FMS wave into the ion cyclotron wave and ion Bernstein wave was calculated as a function of the relative fraction of hydrogen minority varying in the range from 10 to 30%. It turned out that the best absorption of the RF wave by electrons occurs when 24% of hydrogen is added to the deuterium plasma. In this case, electrons absorb approximately 80% of the introduced RF power that can ensure high current drive efficiency of this method. Therefore, this method can be considered promising in terms of using it in experiments at ITER and future fusion reactors. Previously, this method for current drive has not been tested experimentally.

At toroidal facilities with magnetic plasma confinement, experiments on ion cyclotron resonance (ICR) heating of the electron and ion plasma components are ongoing. The ICR heating system introducing power of 9 MW into the plasma has been manufactured at the WEST tokamak [10, 11]. The conversion of the FMS wave into slow waves in deuterium plasma with hydrogen minority is used to organize absorption of the FMS waves. In the experiment, the amount of hydrogen minority in the deuterium plasma varied within the range from 2 to 18%. In this case, the fraction of power, absorbed by plasma electrons, decreased from 67 to 15%, while on the contrary, the fraction of power, absorbed by the plasma ions, increased from 28 to 55%. That is, the experiments conducted at the WEST tokamak showed that by changing the amount of hydrogen minority in deuterium plasma, it is possible to vary the fraction of power absorbed by electrons and thereby, affect the current drive efficiency.

Experiments on studying the effect of phasing the antenna consisting of two current straps on the efficiency of plasma heating were conducted at the EAST tokamak [12]. Power emitted by the antenna was 1.5 MW, and the phase relation of the antenna straps varied from antiphase ($0-\pi$) to almost in-phase ($0-1/3\pi$). In these experiments, the maximum increase in the plasma energy content was observed at the antiphase voltage applied to the antenna straps; the energy

content increased from 120 to 180 kJ. This occurred due to the fact that at such phasing of the antenna straps, the inflow of iron impurity was minimal (the plates of the electrostatic screen are made of stainless steel), and at almost in-phase RF voltage supplied, it was maximal.

For experimentally implementing the MCCD method, the following conditions should be met. First, the waves should propagate in only one of the toroidal directions. Second, the slow waves that occur as a result of mode conversion should be efficiently absorbed by plasma electrons in accordance with the Landau damping mechanism, i.e., the efficient heating of the plasma electron component should be ensured. Before conducting experiments on MCCD, it is necessary to determine the ranges of parameters, in which both of these conditions are met.

In this paper, the satisfability of the first of these conditions at the L-2M stellarator is experimentally studied. Section 2 provides for a brief description of the L-2M facility, at which the experiments were conducted, and describes the two-channel ion cyclotron resonance heating system based on the two-strap antenna, which was used for exciting FMS waves in plasma of the L-2M stellarator. Section 3 describes the system of magnetic probes and data acquisition system that were used in the experiments on measuring the phase velocity of FMS waves. Section 4 presents the experimental results. In Section 5, the main results of the work are summarized.

2. EXPERIMENTAL

The experiments were conducted at the L-2M stellarator, which is a toroidally symmetric magnetic trap designed for confining high-temperature plasma. L-2M is a classical two-turn stellarator (number of helical windings is $l = 2$, number of field periods around the torus is $N = 7$) with the major radius $R =$ 1 m, average plasma radius $a = 0.115$ m and toroidal magnetic field $B_0 = 1–1.4$ T [13]. The rotational transformation angle created by the magnetic system varies from $\iota = 0.18$ at the magnetic axis of the system to $\iota =$ 0.78 at the plasma boundary. In the experiments, hydrogen was used as the working gas. The working range of electron densities is $n_e = (0.2–2.0)\times10^{19}$ m^{-3}. The facility can operate in both the ohmic and electron cyclotron resonance regimes of plasma heating.

In the ohmic heating regime, the plasma current is excited by metal inductor, which is the core of transformer. The plasma current is 10–20 kA. For breaking down the working gas, the loop voltage of approximately 30 V is created. In the L-2M stellarator, the direction of the plasma current always coincides with the direction of the toroidal magnetic field. In this case, the angles of rotational transformation created by the current and magnetic windings are summed, and the total angle of rotational transformation is equal to approximately 1 along most of the plasma radius.

For obtaining stable and long-lasting ohmic discharges with controlled density in the L-2M stellarator, the vacuum chamber walls are boronized in the glow discharge in helium, into which vapors of carborane $C_2B_{10}H_{12}$ are additionally puffed. The carborane vapors dissociate in the discharge, and the chamber walls become covered with boron–carbon film with a thickness of approximately 80 μm. As a result of applying this procedure, in the ohmic heating discharge, the intensities of oxygen and carbon lines decrease by 5 and 3 times, respectively, and the total radiation loss power is reduced by approximately 2.5 times [14].

For exciting FMS waves in plasma of the L-2M stellarator, the two-channel system for ion cyclotron resonance plasma heating based on the two-strap antenna was created. The system consists of the two-channel driving generator, two amplifying lines for supplying RF voltage to the antenna straps, system for matching the antenna circuit and the final amplifier stage (the load of the final amplifier stage should be 50 Ohm), and two straps of the RF antenna [15].

The antenna consists of two current straps located in adjacent cross-sections of the vacuum chamber and spaced by 22.5 cm in the direction along the plasma column axis. The width of each current strap is 7.5 cm, and the surface area is 2.5 dm^2. The plasma-facing surface of each strap repeats the shape of the separatrix surface and is located at a distance of 1 cm from it. The current straps are not protected by electrostatic shield. Each strap is fed by its own amplifier line using a separate RF feeder; therefore, depending on the phase shift between the voltages supplied to individual antenna straps, it is possible to excite FMS waves with different toroidal wave numbers. The vacuum feedthrough devices are assembled based on high-voltage ceramic insulators, which allow supplying RF voltage of up to 15 kV to the antenna. If applying such a voltage to dipole antenna, it can be expected (with allowance for the total area of the antenna system of $S_{an} \approx 0.05$ m^2) that the P_{ICRH} power irradiated by the antenna in experiments on ICR heating of D + H plasma will exceed 100 kW [16].

The Juntek PSG9080 two-channel programmable signal generator (SG) was used as a driving generator of RF signals. This SG provided for generating sinusoidal signals with powers of up to 50 mW at two independent outputs, with the possibility of changing the phase difference between the output signals.

For amplifying the signals of the RF driving generator, two identical two-stage amplification lines were assembled [17]. In the first stage, the U1 power amplifier (manufactured by TZT RF) is used, which had a power gain of 2000 for 1-mW-power input signals. The first stage amplifies the driving generator power to 5 W. The second stage includes the U2 power amplifier (which is PA5 amplifier based on MOSFET tran-

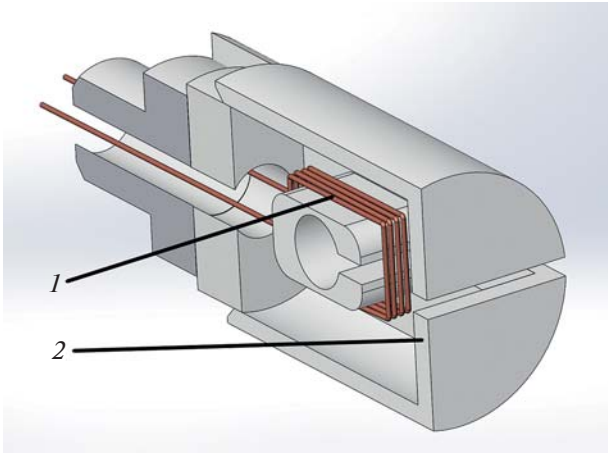

Fig. 1. Design of magnetic probe. (*1*) Probe coil, and (*2*) electrostatic shield.

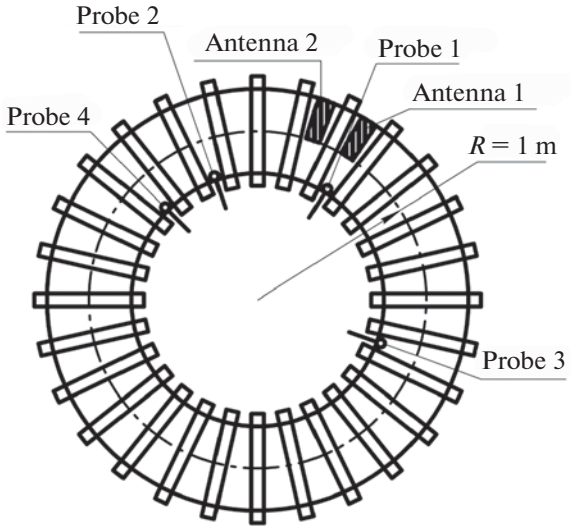

Fig. 2. Arrangement of magnetic probes inside vacuum chamber.

sistors, manufactured by EB104 equipment, with the output power of 1.0 kW and operating frequency range of 1.8–30 MHz) with a power gain of up to 200 for input signals with powers of 5–10 W. RF voltage with power of approximately 1 kW and frequency of 20 MHz is applied to each of the antenna straps; the frequency of 20 MHz corresponds to the ion cyclotron resonance frequency at the axis of the plasma column for the magnetic field of $B_0 = 1.31$ T.

The RF power supplied to the antenna straps was determined using the amplitude meter for the incident and reflected waves. The amplitude meter for the incident and reflected waves is a section of the RF feeder with two conductors inside it, forming two additional distributed lines [16]. The signals from the outputs of additional lines are proportional to the amplitudes of the incident and reflected waves.

3. SYSTEM OF MAGNETIC PROBES AND DATA ACQUISITION SYSTEM FOR MEASURING PHASE VELOCITIES AND DECAY LENGTHS OF FMS WAVES

For measuring the phase velocities of FMS waves, the diagnostics system was created, consisting of a set of magnetic probes and data acquisition equipment based on the LA-n25 oscilloscope cards.

Each magnetic probe is a small (6-mm-diameter) coil of 12 turns, shut with the electrostatic shield (Fig. 1). The core of magnetic probe coil has a length of 4 mm; the cross-sectional area of the core is 20 mm^2 (all probe components are made of stainless steel). The probe inductance is 0.3 μH. The probe is installed at atmospheric pressure, and the cap separates it from the vacuum volume of the L-2M stellarator. This design allows changing the orientation of magnetic probe without disturbing vacuum conditions in the facility.

Four such magnetic probes are installed inside the vacuum chamber in four ports at the inner side of the stellarator chamber at a distance of approximately 10 mm from the plasma boundary (Fig. 2). The axes of the probe coils are directed along the toroidal magnetic field of the stellarator; therefore, the probes measure the longitudinal component of the alternating magnetic field. We note that if the RF plasma heating system was switched off during the OH discharge, the probes recorded the changes in the toroidal magnetic field of the facility The distance along the magnetic axis of the facility between the cross-sections, in which probes *1* and *3* are located, is 135 cm, and for the probes *2* and *4*, it is 45 cm (see Fig. 2). Simulations of the profiles of the FMS wave field components, performed within the framework of the model of cold collisionless plasma, show that near the chamber walls, the B_z component of the FMS wave magnetic field (z is the direction along the toroidal magnetic field) has large amplitude (~1/3 of its maximum value) [18]. Therefore, the magnetic probe placed in the gap between the plasma and the vacuum chamber wall measures the signal corresponding to the B_z component of the FMS wave.

The magnetic probe for measuring FMS waves differs from the conventional Mirnov magnetic probe only in the number of turns. The number of turns in the Mirnov probes is larger by 1–2 orders of magnitude. This is because the Mirnov probes are designed for measuring MHD oscillations that have frequencies of several hundred kilohertz, while probes for measuring FMS waves record magnetic field oscillations with frequencies of several tens of megahertz. Therefore, there is no need in using a larger number of turns to obtain signals sufficient for performing measurements.

In the ohmic heating regime, MHD oscillations make a negligible contribution to the signal of magnetic probe designed for measuring FMS waves. As noted above, in discharges without RF plasma heating, in the ohmic heating regime, signals corresponding to the changes in the toroidal magnetic field are visible, and signals corresponding to MHD oscillations are not visible.

The magnetic probe signal has sinusoidal shape with a frequency equal to the generator frequency. Therefore, only the amplitude and phase of this signal are informative. From the phase correlations between two signals, it is possible to determine the phase velocity of FMS wave, and from the amplitude correlations, the damping length of the wave in the toroidal direction can be calculated. In this work, the phase velocities (longitudinal wave numbers) were measured. The data acquisition system is based on recording signals from two probes installed in the stellarator chamber at different distances from the cross-section of RF power input. The probe signals are recorded using the two-channel LA-n25 oscilloscope card. The digitization frequency of this card can be ν_o = 2.5, 5, 10, or 20 megasamples per second, and the amplitude resolution is 10 bits (2^{10} points). In this work, data reading was performed with a frequency close to the frequency of the wave propagating in plasma. As a result, the beating signal of two frequencies was stored in the computer memory: the frequency of propagating wave and frequency of reading data by the oscilloscope card. It is easy to show that the phase shift of the signals of two probes at the generator frequency is transmitted onto the recorded signals with the beat frequency [19]. Based on the phase shift $\Delta\varphi$ between the signals of two probes spaced by the distance Δl, it is possible to determine the phase velocity of wave propagation in the toroidal direction $V_\varphi = \Delta l/\Delta t$, where $\Delta t = (\Delta\varphi/2\pi)T$, where T is the beat period, and the longitudinal wave number is $k_\parallel = \omega/V_\varphi$.

4. RESULTS AND DISCUSSION

Phase velocities of FMS waves excited by the antenna in plasma of the L-2M stellarator were measured in the ohmic heating regime. The regime with increasing plasma density was organized in order to make it possible to measure the density dependence of the longitudinal wave number of FMS waves in one facility shot. In this case, the plasma current turned out to be decreasing during the shots. However, when studying the propagation of FMS waves in plasma, the key parameters are the density and magnetic field, since the longitudinal wave numbers of waves that can propagate in plasma depend heavily on them. The issues of FMS wave absorption in plasma, for which the electron and ion temperatures are important, were not considered in this paper. Typical shot parameters in this regime are shown in Fig. 3. From top to bottom,

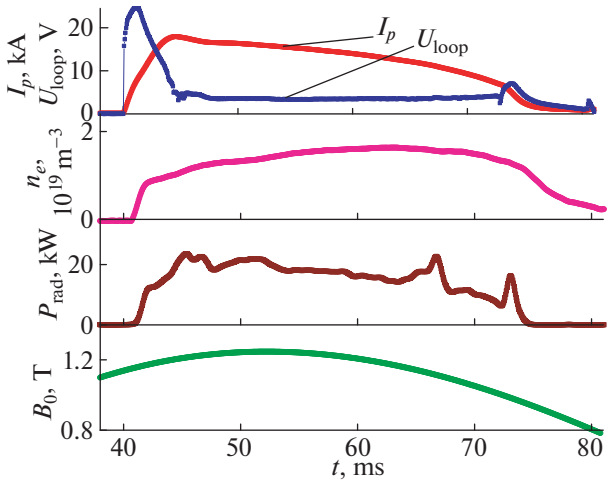

Fig. 3. Typical parameters of L-2M shot in ohmic heating regime. From top to bottom: plasma current $I_p(t)$, loop voltage $U_{loop}(t)$, electron density $n_e(t)$, radiation loss power $P_{rad}(t)$, and magnetic field $B_0(t)$.

the time dependences of the plasma current $I_p(t)$, loop voltage $U_{loop}(t)$, electron density $n_e(t)$, radiation loss power $P_{rad}(t)$, and magnetic field $B_0(t)$ are shown.

In this regime, the signals of four magnetic probes were measured (see Fig. 2). Figure 4 shows the signals of magnetic probes *1* and *3* (Fig. 4a), as well as probes *2* and *4* (Fig. 4b). The modulation on the probe signals can be seen; it occurs as a result of interference of the FMS waves propagating from the antenna in two toroidal directions. In the ohmic heating regime, the loop voltage is applied at the 40th ms. From this time, the plasma density begins to increase. Accordingly, the radiation resistance of the antenna increases, the generator load also increases, and the coupling of the antenna and generator changes. This results in the fact that the amplitudes of the RF voltages supplied to the antenna straps and the probe signals decrease several times, which is illustrated by the signal of probe *1*. In addition, at some time, the conditions arise for the propagation of FMS waves through the plasma in two toroidal directions, co- and counter to the magnetic field direction. Under conditions of weak wave damping, interference of these waves occurs (wave damping is small if the magnetic field inside the facility is less than the ion cyclotron field).

The phase velocities and longitudinal wave numbers were calculated from the phase differences of the sinusoidal signals of the pairs of probes *1*, *3* and *2*, *4*. This made it possible to measure the density dependence of the longitudinal wave number in the L-2M stellarator. Figure 5 shows the dependences measured from the signals of the pairs of probes *1*, *3* and *2*, *4* at the magnetic field of B_0 = 1.25 T. Curve *1* was obtained in the case of exciting the FMS wave by the two-strap antenna with the straps phasing (0–π) when 1 kW of

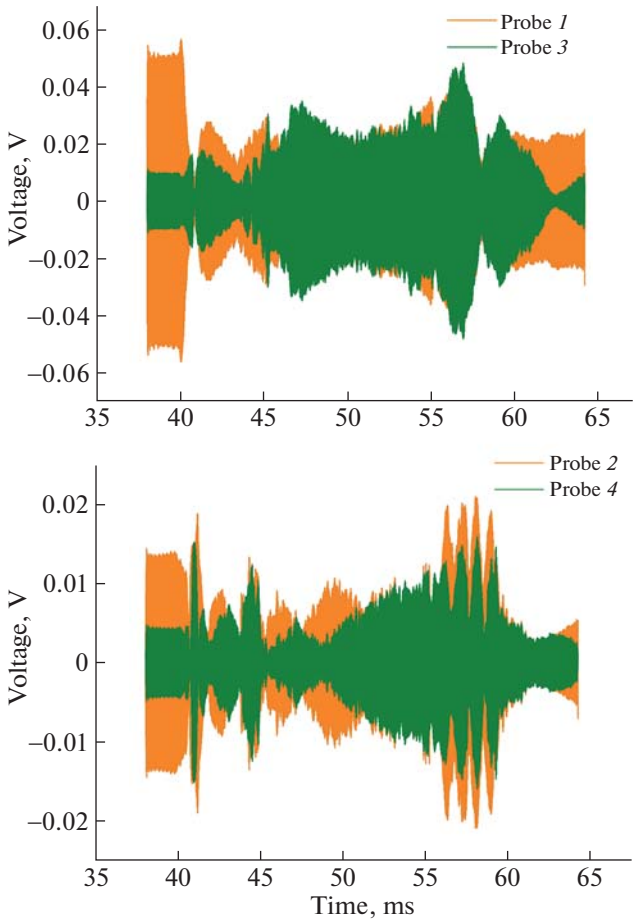

Fig. 4. Signals of magnetic probes (a) (*1, 3*) and (b) (*2, 4*).

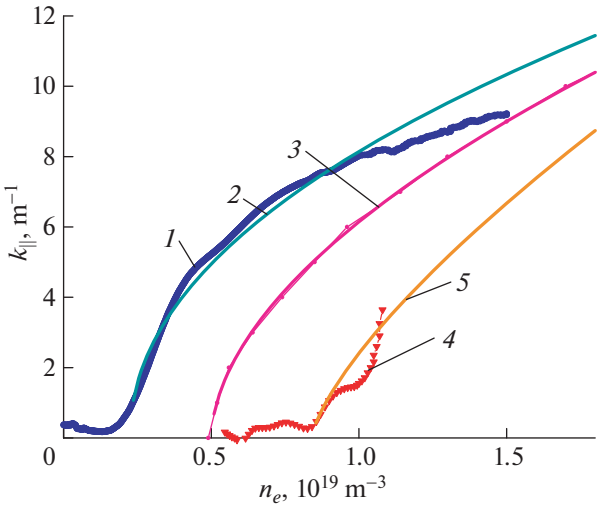

Fig. 5. Longitudinal wave number of FMS wave as a function of plasma density at magnetic field $B_0 = 0.95\ B_{ci}$. (*1*) Experimental dependence for wave propagating counter to toroidal magnetic field in stellarator (from probe *1* to probe *3*); (*2*) approximation of dependence (*1*); (*3*) dependence calculated using model of cold collisionless plasma; (*4*) experimental dependence for wave propagating in direction of toroidal magnetic field (from probe *2* to probe *4*); and (*5*) approximation of dependence (*4*).

RF power was supplied to the straps. Curve *4* was obtained in the case exciting the FMS wave by single-strap antenna *2* when 0.5 kW of RF power was supplied to it. The dependences were approximated by curves *2* and *5*, respectively. Curve *3* represents the dependence of the longitudinal wave numbers of the FMS wave on the average plasma density calculated within the framework of the model of cold collisionless plasma for cylindrical geometry [20]. The calculations were performed for the azimuthal wave number $m = 1$, since this is the only azimuthal mode that can be excited in the L-2M stellarator plasma in the range of operating densities [19]. The figure shows that in the experiment, the FMS waves propagating in the directions along and against the toroidal magnetic field are characterized by different $k_{\|}(n_e)$ dependences, none of which coincides with calculated dependence *3*, which turned out to be between them. When calculating curve *3*, the cylindrical model was used, in which the plasma was considered homogeneous along the z and φ coordinates. Under these conditions, the waves, which are solutions to the dispersion equation, propagate with the same phase velocity in both directions with respect to the toroidal magnetic field. In the experiment, the plasma density is non-uniform along the azimuthal angle φ, as well as the structure of the magnetic surfaces. Apparently, this leads to unalike conditions for the propagation of FMS waves in two toroidal directions: co- and counter to the direction of the magnetic field. Therefore, curve *3* does not coincide with any of the experimental curves *1* or *4*. In addition, in the calculations, the poloidal component B_φ of the magnetic field causes small splitting of the $k_{\|}(n_e)$ dependence for the FMS wave [21]. In the experiment, very strong splitting of the density dependences of the longitudinal wave number is observed, which, in the authors' opinion, is associated with the azimuthal rotation of the elliptical plasma cross-section when moving around the torus. We note that FMS waves propagating in the directions along and against the magnetic field have different density thresholds for their excitation. When FMS waves propagate in the direction against the magnetic field, the density threshold at the magnetic field of $B_0 = 1.25$ T is $n_e = 0.2 \times 10^{19}$ m^{-3}. At the same time, for the FMS wave propagating in the direction along the magnetic field, the density threshold at the same magnetic field is $n_e = 0.8 \times 10^{19}$ m^{-3}.

The density dependences of the longitudinal wave number were also measured at other magnetic fields in the range of $B_0 = 1$–1.4 T. Figure 6 shows two dependences for magnetic fields $B_0 = 1.1$ (0.84 B_{ci}) and 1.33 T (1.01 B_{ci}), where B_{ci} is the cyclotron magnetic

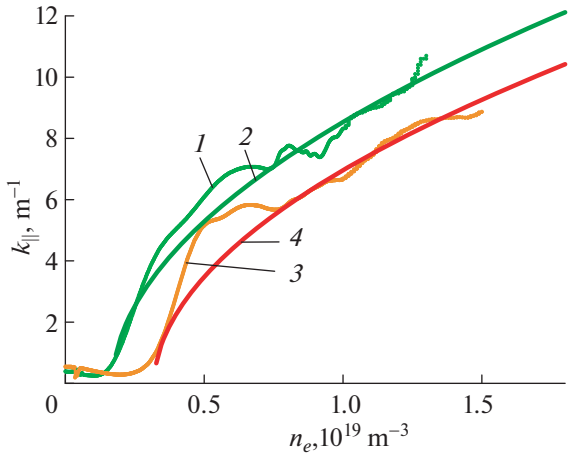

Fig. 6. Longitudinal wave numbers of FMS waves propagating counter to toroidal magnetic field in stellarator (from probe *1* to probe *3*) as functions of plasma density at two magnetic fields. $B_0 = (1, 2)\ 0.84B_{ci}$ and $(3, 4)\ 1.01B_{ci}$. (*1*, *3*) Experimental results and (*2*, *4*) approximations of experimental curves.

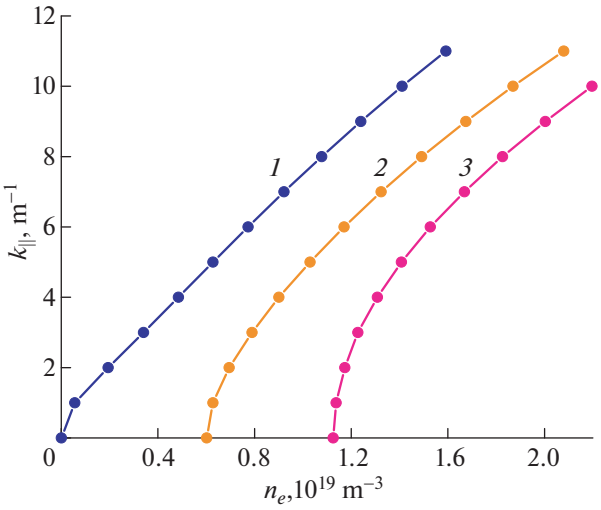

Fig. 7. Calculated dependences of longitudinal wave numbers of FMS waves on density for three toroidal magnetic fields in stellarator. (*1*) $B_0 = 0.85\ B_{ci}$, (*2*) $B_0 = 0.95\ B_{ci}$, and (*3*) $B_0 = B_{ci}$.

field for hydrogen ions. It is evident that for any fixed density, with an increase in the magnetic field at the facility axis, there occurs a decrease in the longitudinal wave numbers of FMS waves, which can propagate in plasma of the L-2M stellarator. In addition, with an increase in the magnetic field, the density threshold for the excitation of FMS waves increases. This agrees with the calculations performed within the framework of the model of cold collisionless plasma for cylindrical geometry. Figure 7 shows the calculated dependences $k_{\|}(n_e)$ for three magnetic fields B_0 = 1.1, 1.25, and 1.33 T.

From the point of view of the planned experiments on current drive using FMS waves, FMS waves propagating in the same direction as the plasma current, i.e., in the direction along the magnetic field, are of interest. In the experiments under consideration, 0.5 kW of RF power was supplied to the single-strap antenna. Using probes *2* and *4*, the $k_{\|}(n_e)$ dependence was measured at two magnetic fields B_0 = 1.25 and 1.32 T (Fig. 8, curves *1* and *3*, respectively). The figure also shows approximations of the experimental curves (curves *2* and *4*, respectively). Figure 8 shows that for the FMS waves propagating along the toroidal magnetic field, the changes in the $k_{\|}(n_e)$ dependences with increasing magnetic field are similar to those in the case of FMS waves propagating counter to the magnetic field. Namely, with an increase in the magnetic field, the longitudinal wave number of the FMS wave excited at a given density decreases, and the density threshold for its excitation increases.

As can be seen in Fig. 6, at low densities, the measured $k_{\|}(n_e)$ dependences considerably deviate from the approximating curves. These deviations are non-random. In support of this statement, Fig. 9 shows the $k_{\|}(n_e)$ dependences measured at the L-2M stellarator previously [19]. It is evident that all the curves in Fig. 9 have similar deviations. They are associated with the changes in density profile in the initial stage of the discharge. In the stage of density ramp-up, the shape of the density profile highly differs from its shape in the quasi-stationary stage. At the beginning of discharge, the shape of the density profile is very sharp. Unfortunately, in this experiment it was not possible to mea-

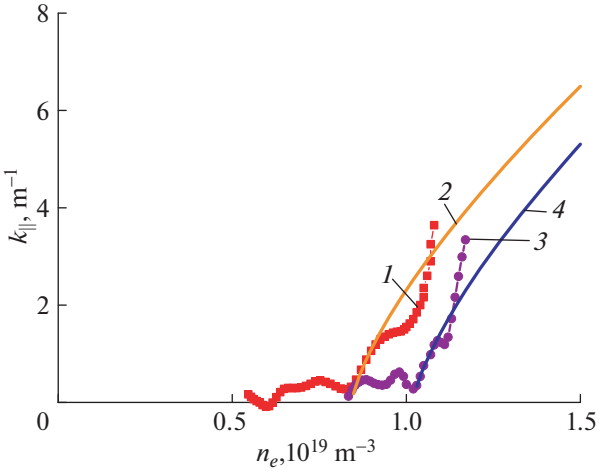

Fig. 8. Longitudinal wave numbers of FMS waves propagating in direction of toroidal magnetic field in stellarator (from probe *2* to probe *4*) as functions of plasma density at two magnetic fields: (*1*) $B_0 = 0.95B_{ci}$, and (*3*) $B_0 = B_{ci}$. (*1*, *3*) Experimental results and (*2*, *4*) approximations of experimental curves.

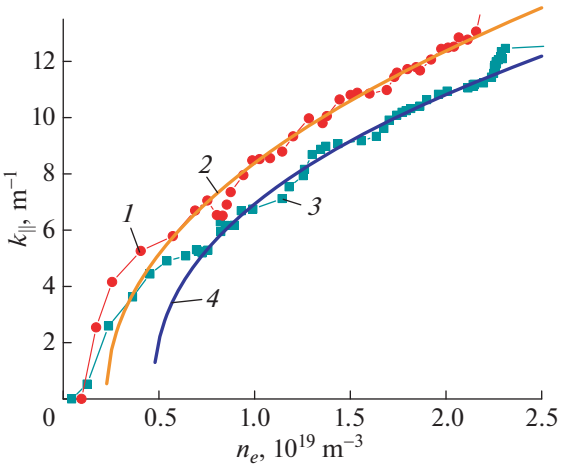

Fig. 9. Longitudinal wave numbers of FMS waves propagating counter to toroidal magnetic field in stellarator (from probe *1* to probe *3*) as functions of plasma density at two magnetic fields. $B_0 = (1, 2)\ 0.9B_{ci}$ and $(3, 4)\ 0.95B_{ci}$. (*1*, *3*) Experimental results and (*2*, *4*) approximations of experimental curves. Dependences were measured previously at the L-2M stellarator in ohmic heating regime [18].

sure the radial profiles of the plasma density; therefore, the effect of the shape of density profile on the $k_{\|} = f(n_e)$ dependence was estimated only based on the results of calculations performed within the framework of the cylindrical one-dimensional model.

5. CONCLUSIONS

The system of magnetic probes and data acquisition system have been designed and created at the L-2M stellarator for measuring phase velocities of FMS waves excited in plasma. Using this system of magnetic probes, toroidal and azimuthal wave numbers of FMS waves excited in the L-2M stellarator plasma were determined in the ohmic heating regime at 1-kW-power of radiation introduced into the plasma, plasma densities in the range of $(0.5–2.0) \times 10^{19}$ m^{-3} and magnetic fields in the range of 1–1.4 T.

It was shown that at plasma densities higher than 1.0×10^{19} m^{-3} in the ohmic heating regime of the L-2M stellarator operation, FMS waves can be excited that propagate in two toroidal directions: along and against the direction of the toroidal magnetic field. Density thresholds for excitation of FMS waves propagating in both directions were determined. From the point of view of the planned experiments on current drive using FMS waves, the FMS waves propagating in the same direction as the plasma current, i.e. along the magnetic field, are of interest. The density threshold for excitation of this FMS waves is 1.0×10^{19} m^{-3} at the magnetic field equal to the ion cyclotron field. With decreasing magnetic field, the density threshold for excitation of FMS waves in the direction of the magnetic field decreases. For FMS waves propagating in the direction counter to the magnetic field, the density threshold for the excitation of FMS waves is 0.3×10^{19} m^{-3} at the magnetic field equal to the ion cyclotron field, and it also decreases with decreasing magnetic field. Thus, in the ohmic heating regime in the density range of $(0.3–1.0) \times 10^{19}$ m^{-3}, for the magnetic field equal to the ion cyclotron field, there are conditions, under which FMS waves excited in plasma of the L-2M stellarator can propagate in only one of the toroidal directions.

FUNDING

The work was supported by the Ministry of Science and Higher Education of the Russian Federation under the State Contract FFWF-2025-0002.

CONFLICT OF INTEREST

The authors of this work declare that they have no conflicts of interest.

OPEN ACCESS

REFERENCES

1. K. Ushigusa, JAERI Report 1339 (Japan Atomic Energy Research Institute, Tōkai, 1999).
2. O. Naito and JT-60 Team, Plasma Phys. Controlled Fusion **35**, B215 (1993). https://doi.org/10.1088/0741-3335/35/SB/017
3. I. H. Hutchinson, R. Boivin, F. Bombarda, P. Bonoli, S. Fairfax, C. Fiore, J. Goetz, S. Golovato, R. Granetz, M. Greenwald, S. Horne, A. Hubbard, J. Irby, B. LaBombard, B. Lipschultz, et al., Phys. Plasmas **1**, 1511 (1994). https://doi.org/10.1063/1.870701
4. V. V. Alikaev, A. A. Bagdasarov, A. A. Borshegovskij, V. V. Chistyakov, M. M. Dremin, Yu. A. Gorelov, A. V. Gorshkov, Yu. V. Esipchuk, D. B. Evdokimov, A. Ya. Kislov, D. A. Kislov, V. A. Krupin, L. K. Kuznetsova, S. E. Lysenko, G. E. Notkin, et al., Nucl. Fusion **35**, 369 (1995). https://doi.org/10.1088/0029-5515/35/4/I01

5. C. C. Petty, R. Prater, J. Lohr, T. C. Luce, W. R. Fox, R. W. Harvey, J. E. Kinsey, L. L. Lao, and M. A. Makowski, Nucl. Fusion **42**, 1366 (2002). https://doi.org/10.1088/0029-5515/42/12/303
6. C. C. Petty, F. W. Baity, J. S. deGrassie, C. B. Forest, T. C. Luce, T. K. Mau, M. Murakami, R. I. Pinsker, P. A. Politzer, M. Porkolab, and R. Prater, Nucl. Fusion **39**, 1421 (1999).
7. R. Majeski, J. H. Rogers, S. H. Batha, R. Budny, E. Fredrickson, B. Grek, K. Hill, J. C. Hosea, B. LeBlanc, F. Levinton, M. Murakami, C. K. Phillips, A. T. Ramsey, G. Schilling, G. Taylor, et al., Phys. Rev. Lett. **76**, 764 (1996). https://doi.org/10.1103/PhysRevLett.76.764
8. L. Yin, C. Yang, X. Y. Gong, X. Q. Lu, D. Du, and Y. Chen, Phys. Plasmas **24**, 102502 (2017). https://doi.org/10.1063/1.5002137
9. L. Yin, C. Yang, X. Y. Gong, X. Q. Lu, J. J. Cao, Z. Y. Wu, Y. Chen, and D. Du, AIP Adv. **8**, 055315 (2018). https://doi.org/10.1063/1.5018661
10. C. Bourdelle, J. F. Artaud, V. Basiuk, M. Bécoulet, S. Brémond, J. Bucalossi, H. Bufferand, G. Ciraolo, L. Colas, Y. Corre, X. Courtois, J. Decker, L. Delpech, P. Devynck, G. Dif-Pradalier, et al., Nucl. Fusion **55**, 063017 (2015). https://doi.org/10.1088/0029-5515/55/6/063017
11. P. Huynh, E. A. Lerche, D. Van Eester, J. F. Artaud, R. Dumont, P. Maget, P. Manas, and WEST Team, Fusion Eng. Des. **205**, 114549 (2024). https://doi.org/10.1016/j.fusengdes.2024.114549
12. L. N. Liu, Q. C. Liang, H. Yang, X. J. Zhang, S. Yuan, Y. Z. Mao, W. Zhang, G. H. Zhu, L. Wang, C. M. Qin, Y. P. Zhao, Y. Cheng, and K. Zhang, Nucl. Eng. Technol. **54**, 3614 (2022). https://doi.org/10.1016/j.net.2022.05.030
13. V. V. Abrakov, D. K, Akulina, E. D. Andryukhina, G. M. Batanov, M. S. Berezhetskij, I. S. Danilkin, N. P. Donskaya, O. I. Fedyanin, G. A. Gladkov, S. E. Grebenshchikov, J. H. Harris, N. K. Kharchev, Yu. V. Kholnov, L. V. Kolik, L. M. Kovrizhnykh, et al., Nucl. Fusion **37**, 233 (1997). https://doi.org/10.1088/0029-5515/37/2/I08
14. A. I. Meshcheryakov, D. K. Akulina, G. M. Batanov, M. S. Berezhetskii, G. S. Voronov, G. A. Gladkov, S. E. Grebenshchikov, V. A. Grinchuk, I. A. Grishina, L. V. Kolik, N. F. Larionova, A. A. Letunov, V. P. Logvinenko, A. E. Petrov, A. A. Pshenichnikov, et al., Plasma Phys. Rep. **31**, 452 (2005); https://doi.org/10.1134/1.1947330
15. A. I. Meshcheryakov, I. A. Grishina, and I. Yu. Vafin, Plasma Phys. Rep. **48**, 1049 (2022). https://doi.org/10.1134/S1063780X22600451
16. A. I. Meshcheryakov, I. A. Grishina, and I. Yu. Vafin, Instrum. Exp. Tech. **65**, 774 (2022). https://doi.org/10.1134/S002044122205027X
17. A. I. Meshcheryakov, I. A. Grishina, and M. E. Popov, Instrum. Exp. Tech. **68** (4), 2025 (in press).
18. A. I. Meshcheryakov, A. E. Morozov, A. A, Golikov, I. Yu. Vafin, M. S. Berezhetskii, and I. Yu. Nechaev, Prikl. Fiz., No. 6, 51 (2007).
19. A. I. Meshcheryakov, I. Yu. Vafin, A. E. Morozov, A. A. Golikov, and I. Yu. Nechaev, Plasma Phys. Rep. **34**, 203 (2008). https://doi.org/10.1134/S1063780X08030069
20. A. I. Meshcheryakov and I. A. Grishina, Instrum. Exp. Tech. **68** (4), 2025 (in press).
21. A. I. Meshcheryakov, PhD Thesis (General Physics Institute of the Russian Academy of Sciences, Moscow, 1993).

Translated by I. Grishina